

# Spin Relaxation in Nematogens and their Deuterated Derivatives

Ronald Y. Dong

Department of Physics and Astronomy  
Brandon University  
Brandon, Manitoba, Canada

## I. INTRODUCTION

A brief review of spin relaxation (1) in nematogens is given. The usual problems in this area arise from the lack of a good theoretical model and a spin system in which meaningful measurements and direct comparison with the model can be made. The proton and deuteron spin-lattice relaxation in nematics have been extensively studied both theoretically (2,3) and experimentally (4-8). It is generally agreed that the total proton relaxation rate is the sum of two contributions

$$T_{1 \text{ total}}^{-1} = T_{1a}^{-1} + T_{1r}^{-1} \quad (1)$$

where  $T_{1a}^{-1}$  is an intramolecular contribution and  $T_{1r}^{-1}$  an intermolecular contribution. They are due to the modulation of the dipolar interactions within a molecule and between different molecules, respectively. The deuteron relaxation rate is governed by the modulation of the electric quadrupole interactions which are almost entirely intramolecular.

Recent theoretical studies (2,3) have shown that the intramolecular relaxation is a sum of three contributions, *viz*, nematic order director fluctuations,  $T_{1 \text{ odf}}^{-1}$ , angular fluctuations of the long molecular axis

about the short molecular axis,  $T_{1 \text{ afs}}^{-1}$ , and a coupling between the former two contributions to provide a cross-relaxation,  $T_{1 \text{ cross}}^{-1}$ . Both theories give identical expressions for  $T_{1 \text{ odf}}^{-1}$  and  $T_{1 \text{ afs}}^{-1}$ , but different expressions for  $T_{1 \text{ cross}}^{-1}$ . The cross-relaxation term in the theory of Doane and co-workers (2) is always positive and often the dominant term. It also remains finite even in the isotropic limit where the order parameter  $S$  becomes zero. On the other hand, the theory of Freed (3) gives a cross-relaxation term which is negative and dependent on the effect of cutoff. It is often smaller than the other two terms. Furthermore, the cross-relaxation becomes zero when  $S$  becomes zero, as one would expect for an isotropic liquid. An earlier spin-lattice relaxation study (6) of the partially deuterated *p*-azoxyanisole (PAA) and *p*-methoxybenzylidene-*p*-*n*-butylaniline (MBBA) met with limited success when Doane's theory was applied, probably due to the improper cross-relaxation term. Here we choose Freed's theory to re-examine some previous proton and deuteron data. Freed has also considered (3) the intramolecular spin relaxation by quasi-critical order parameter fluctuations (OPF) which may become a dominant relaxation mechanism near the isotropic-nematic phase transition at  $T_c$ . His theory was used

(9) to search for OPF in a study of proton spin-lattice relaxation time ( $T_{1\rho}$ ) in the rotating frame.

Although there is general agreement in the literature on the mechanisms giving rise to the intramolecular relaxation, there is disagreement concerning the mechanisms responsible for intermolecular relaxation. Two recent theories (2,10) of spin relaxation by intermolecular interactions were proposed for liquid crystals. Doane and co-workers (2) adapted their expression for intramolecular relaxation to the intermolecular case by assuming that a pair of spins reside on two perfectly parallel rod-like molecules. The dipolar interaction is again modulated by ODF and AFS, but is turned on or off with a characteristic time  $\tau_d$ , a molecular jump correlation time. As in the intramolecular case, the intermolecular cross-relaxation term is usually large, positive, and finite even in the limit when  $S$  goes to zero. Here we ignore the intermolecular cross-relaxation term. The other theory proposed by Zumer and Vilfan (10) is an extension of Torrey's treatment of isotropic self-diffusion in simple liquids to the anisotropic self-diffusion in liquid crystals. The theory assumes an elongated cylindrical shape for the liquid crystal molecules, a certain distribution of spins on the cylindrical surface, and a perfect alignment of the long molecular axis. As each of these two theories assumes that the relaxation mechanisms treated by the other do not exist, it may be that both are responsible for intermolecular spin relaxation (8) in liquid crystals.

## II. INTRAMOLECULAR CONTRIBUTION

### A. Proton Relaxation

As Freed's theory is applicable to a pair of spin  $-1/2$  nuclei, the appropriate spin system for direct comparison with the theoretical model is the phenyl protons of a suitably deuterated nematogen. Two such nematogens are available to us, *viz.*: methyl-deuterated PAA (PAA- $d_6$ ) and *p*-methoxy- $d_3$ -benzylidene- $d_1$ -*p*-*n*-butyl- $d_9$ -aniline (MBBA- $d_{13}$ ). According to Freed, the proton intramolecular relaxation rate in the laboratory frame is

$$T_{1a}^{-1} = T_{1ODF}^{-1} + T_{1AFS}^{-1} + T_{1CROSS}^{-1} \quad (2)$$

where

$$T_{1ODF}^{-1} = (9/32\sqrt{2\pi})(\gamma^2\hbar/r^3)^2 (1 - 3\cos^2\theta)^2 S^2 \quad (3)$$

$$kTu(\omega/\omega_c)/K(K/\eta + D)^{1/2}\omega^{1/2}$$

$$T_{1AFS}^{-1} = (3/2)(\gamma^2\hbar/r^3)^2 \tau_R [1 - S(1 + 3\cos 2\theta)/4] \quad (4)$$

where the short correlation time limit ( $\tau_R \ll 1/\omega$ ) is assumed.

$$T_{1CROSS}^{-1} = -T_{1ODF}^{-1} (2\sqrt{2}/\pi)(\omega\omega_c)^{1/2}\tau_R/u(\omega/\omega_c) \quad (5)$$

and

$$u(\omega/\omega_c) = 1 - (1/2)\pi\ln\{1 + \sqrt{2}\omega/\omega_c + \omega/\omega_c\}/(1 - \sqrt{2}\omega/\omega_c + \omega/\omega_c) - (1/\pi)\tan^{-1}[\sqrt{2}\omega/\omega_c/(1 - \omega/\omega_c)] + \rho$$

with  $\rho = 0$  if  $(\omega/\omega_c) < 1$ ;  $\rho = 1$  if  $(\omega/\omega_c) > 1$ . Here  $\omega_c/2\pi$  is the critical cutoff frequency which is related to the critical wavelength  $\lambda$ , the average elastic constant  $K$ , and the viscosity  $\eta$  as follows

$$\omega_c = K4\pi^2/\lambda^2\eta \quad (6)$$

In our calculations, we assumed  $\lambda = 25 \text{ \AA}$ , the approximate molecular length. The other quantities in the above equations are:  $\theta$ , the angle between  $r$  and the long molecular axis  $M$ ;  $D$ , the average diffusion coefficient, and  $\tau_R$ , the correlation time for molecular reorientation about the short axis.

Since the measured proton relaxation rate is the sum of  $T_{1a}^{-1}$  and  $T_{1r}^{-1}$ , one must separate them before comparing results with theoretical predictions. This can be achieved reliably by the isotopic dilution technique (11) where one measures the proton relaxation of a partially deuterated molecule in a solution of its perdeuterated analogue, extrapolates the measurements to infinite dilution, and obtains the intramolecular relaxation directly. This was carried out (11) for PAA- $d_6$  at  $120^\circ\text{C}$ . The result is reproduced in Figure 1.

The plot of  $T_{1a}^{-1}$  vs  $\nu^{-1/2}$  indicates that  $\omega\tau_R \ll 1$ . Although the cutoff frequency is 1100 MHz ( $K = 7.8 \times 10^{-7}$  dynes,  $\eta = 7.1 \times 10^{-2}$  poise),  $u(\omega/\omega_c)$  is 0.91 and 0.73 at 10 and 100 MHz, respectively. The experimental data are fitted to Eq. 2 ( $D = 3.4 \times 10^{-6}$  cm<sup>2</sup>/s,  $S = 0.5$ ,  $\theta = 10^\circ$ ). The cross relaxation term is 10% of the AFS contribution, but is comparable in magnitude to the ODF term at 100 MHz and higher frequencies. The ODF contributes only about 24% of the total intramolecular relaxation rate at 60 MHz. The solid curve is drawn for  $r = 2.49 \text{ \AA}$  and  $\tau_R = 1.9 \times 10^{-10}$  s. The deduced value of  $r$  compares well with the accepted value of 2.45  $\text{\AA}$  for a pair of ortho phenyl protons. Dipole-relaxation experiments in PAA at  $125^\circ\text{C}$  give

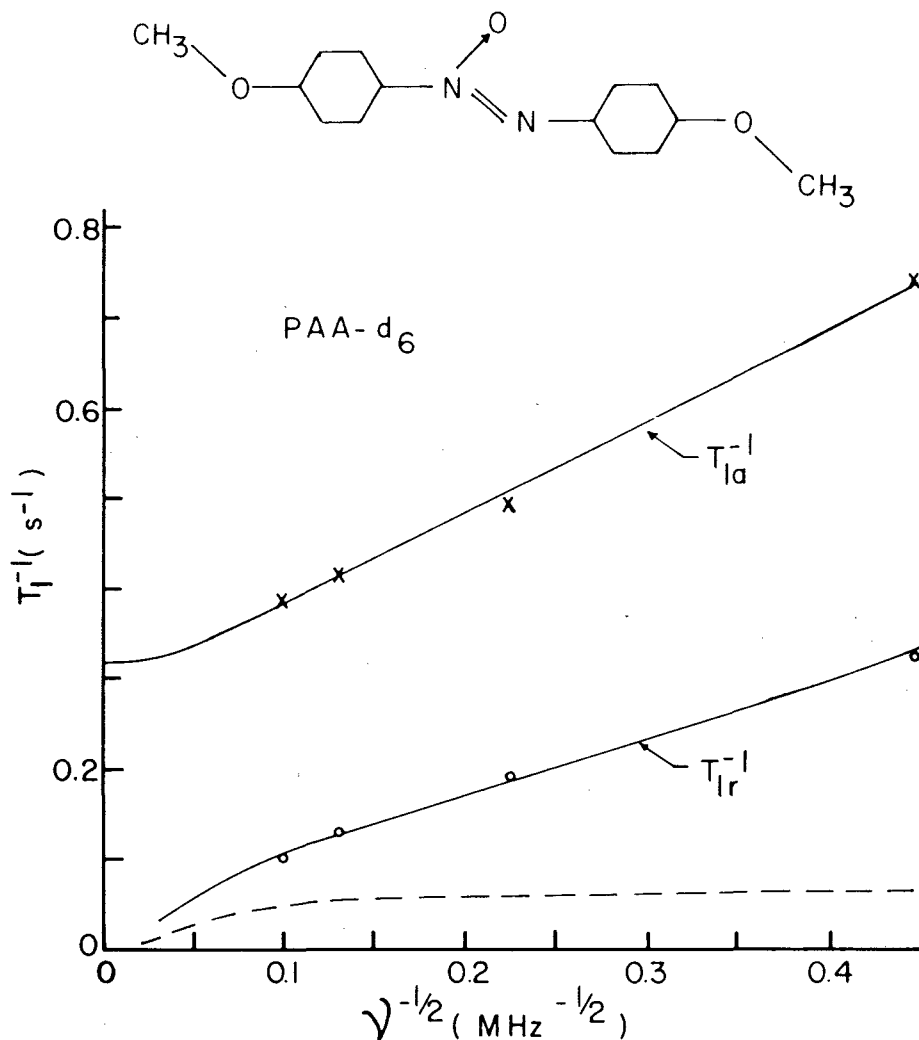


**Figure 1.** The structure of PAA and proton spin-lattice relaxation rate of PAA-d<sub>6</sub> vs inverse square root of the Larmor frequency at 120°C. O and X denote the *inter* molecular and the *intra* molecular contributions, respectively, obtained by Fung *et al*(11). Solid curves denote theoretical plots (see text), and dashed curve is given by the theory of Zumer and Vilfan (10).

two values of  $\nu_D$  for the rotational motion of the long molecular axis:

$$\tau_{D1} = 2.5 \times 10^{-11} \text{ s and } \tau_{D2} = 4.3 \times 10^{-9} \text{ s. } 3\tau_R$$

is an order of magnitude smaller than  $\tau_{D2}$  which is for an end-for-end flip of the molecule. This is reasonable because the large angle fluctuations of

the long molecular axis about the short axis could occur more frequently. The proton  $T_{1a}^{-1}$  has not been measured in MBBA-d<sub>13</sub> by the isotopic dilution method. However, if  $\tau_R$  is determined by other means, one can calculate the theoretical intramolecular contribution to the total proton relaxation in MBBA-d<sub>13</sub>. We will see below that  $\tau_R$  (Table 1)

Table 1.  $\tau_R$  for the Deuterons of Carbon-15 and  $\nu_{D2}$  in MBBA

T (K)	$\tau_R^*$ ( $\times 10^{-10}$ s)	$\nu_{D2}^{**}$ ( $\times 10^{10}$ s)
311	1.1 (1.2)	3
305	1.3 (1.2)	4.8
298	1.7 (1.6)	8.2
289	2.5 (1.7)	19

\* The numbers in parentheses were calculated (7) with  $u(\omega/\omega_c) = 1$  and without the cross-relaxation term.

\*\* F. Rondelez and A. Mircea-Roussel, *Mol. Cryst. Liq. Cryst.* 28, 173 (1974).

can be calculated from the relaxation rate ( $T_{1Q}^{-1}$ ) of C-15 deuterons (see Figure 3). We chose the deuterons on carbon 15 because this carbon atom is situated more or less on the long molecular axis and it is the motion of the long molecular axis which gives rise to the intramolecular relaxation of the phenyl protons. The theoretical proton  $T_{1a}^{-1}$  for MBBA- $d_{13}$  (8) at different frequencies obtained from the calculated values of  $\tau_R$  is reproduced in Figure 2. The experimental proton  $T_{1a}^{-1}$ , when available, would be useful for checking the assumption that the same mechanisms (AFS) which are responsible for the in-

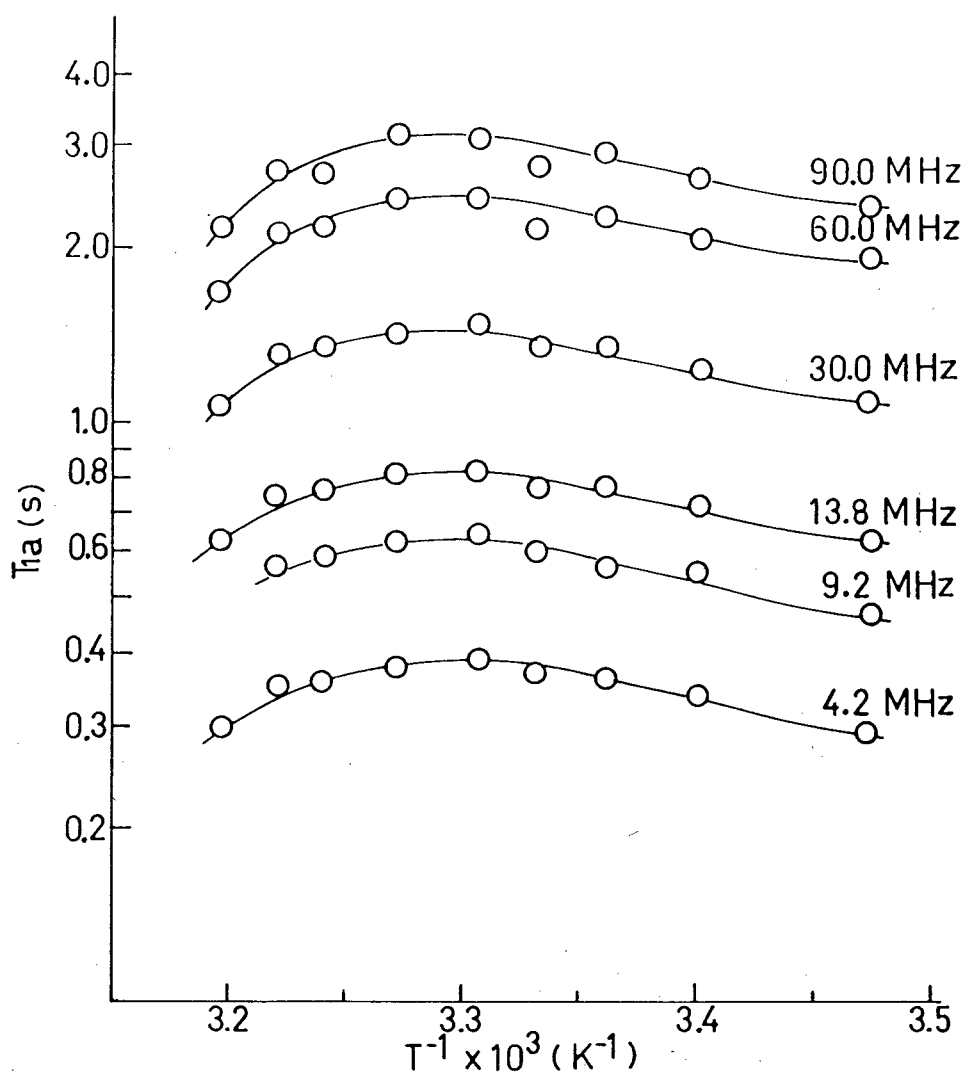


Figure 2. Calculated *intra* molecular proton relaxation time of MBBA- $d_{13}$  at different temperatures and frequencies.

tramolecular relaxation of the phenyl protons are also responsible for relaxing the deuterons on C-15.

## B. Deuteron Relaxation

Eqs. 3-5 are also applicable to the deuteron relaxation, except that the factor  $\gamma^2 \hbar / r^3$  must be replaced with  $e^2 q Q / 2h$  and the angle  $\theta$  is now the angle between the C-D bond and M. There are, however, two problems in using Eq. 3 to calculate the ODF contribution for deuterons. The first problem is that the ODF contribution depends on  $S$  and on the secondary or asymmetry parameter  $\delta$ , which is usually small but unknown. The second problem is that the value of the angular function  $(1 - 3\cos^2\theta)$  is very sensitive to the choice of  $\theta$ , especially in the vicinity of  $\theta = 60^\circ$ . Fortunately, the quadrupole splitting for deuterons,  $\Delta\nu$ , depends on  $\delta$  and  $\theta$  in the same way as the ODF contribution. In terms of  $\Delta\nu$ , the expression for the ODF contribution becomes (7)

$$T_{1ODF}^{-1} = (\Delta\nu)_2 (\pi/2\sqrt{2}) kT u(\omega/\omega_c) / K(D + K/\eta)^{1/2} \omega^{1/2} \quad (7)$$

Deuteron spin-lattice relaxation ( $T_{1Q}$ ) in ring-deuterated PAA—PAA-d<sub>8</sub>—(12) and in ring-deuterated MBBA—MBBA-d<sub>8</sub>—(6,13) shows no detectable frequency dependence between 4 and 45 MHz but a strong temperature dependence. The deuterium spectrum of MBBA-d<sub>13</sub> at 13.81 MHz has the advantage of being well resolved, thus allowing selective deuteron  $T_{1Q}$  measurements (7). A typical spectrum with assignment by the structural carbon numbers is given in Figure 3. In addition, the time-averaged quadrupole tensor along the director is readily determined from the spectrum. In accordance with Eq. 7,  $T_{1ODF}^{-1}$  was calculated for the C-15 deuterons using their  $\Delta\nu$  values (see Figure 4),  $\omega_c = 4.8 \times 10^8 \text{ s}^{-1}$ , and the values for  $K$ ,  $D$ , and  $\eta$  from the literature (14). Subtraction of  $T_{1ODF}^{-1}$  from the measured relaxation rate (Figure 4) yielded the sum of the AFS and CROSS terms, from which the value of  $\tau_R$  (7,8) was finally calculated. In the latter calculation, we use  $\theta = 75^\circ$ , 170 kHz for the quadrupole coupling constant  $e^2 q Q / h$ , and the  $S$  values of Lee *et al* (14). Some  $\tau_R$  values at different temperatures are tabulated in Table 1 together with those obtained in (7) in which both  $u(\omega/\omega_c)$  and cross-relaxation terms are neglected. The assumptions made in (7) are justified, as seen in Table 1. This is because both

the ODF and the cross-relaxation terms for deuterons are small, about 16%, and 1%, respectively, of the AFS contribution for the C-15 deuterons. Also shown in Table 1 are the dielectric relaxation times  $\tau_{D2}$  for MBBA.  $3\tau_R$  is again smaller than  $\tau_{D2}$  as in PAA, but by two orders of magnitude.

Figure 5 shows the deuteron data (6,13) for MBBA-d<sub>8</sub>. We assume again that the  $\tau_R$ 's used above describe the AFS contribution of the phenyl deuterons. The solid line denotes calculations based on the theory of Freed. We used  $\Delta\nu = 10.4 \text{ kHz}$  (for peak *b*) (13) at  $26^\circ\text{C}$  and 13.8 MHz and  $\theta = 58.35^\circ$  to calculate the ODF contribution and  $\theta = 58.35^\circ$ . This angle is also used to calculate the AFS term with  $e^2 q Q / h = 187 \text{ kHz}$ . Since the ODF and CROSS terms constitute about 1-2% of the AFS term,  $T_{1Q}$  should be almost totally independent of frequency. The discrepancies between theory and experiment in the magnitude of  $T_{1Q}$  can be explained by rotation of the ring about its para axis, which produces additional relaxation of phenyl deuterons. As seen in Figure 5, the AFS and ring rotation about the para axis contribute about equally to the observed deuteron relaxation rate in MBBA-d<sub>8</sub>. It was noted that the aniline and benzylidene rings reorient at different rates about the para axes (13).

## C. Order Parameter Fluctuation

Just below  $T_c$ , fluctuations in the magnitude of the nematic order parameter  $S$  may be observable by NMR relaxation techniques. When the quasi-critical OPF contribution dominates over the usual ODF contribution near  $T_c$ , then  $T_{1ODF}^{-1}$  in Eqs. 2 and 5 are replaced by  $T_{1OPF}^{-1}$  (3). To obtain  $T_{1CROSS}^{-1}$  in Eq. 5, we have included  $u(\omega/\omega_c)$  and  $\omega\tau_0 \gg 1$  in  $T_{1OPF}^{-1}$  (see Eq. 8 below) and used  $\omega\tau_R \ll 1$  and  $\omega_c\tau_0 \ll 1$ , where  $\tau_0 \equiv v_N/A$ ,  $A \propto (T - T_c)$  in the mean field approximation, and  $T$  ( $> T_c$ ) is the temperature at which a second order isotropic nematic phase transition would occur. While  $T_{1AFS}^{-1}$  is again given by Eq. 4, Freed (3) has obtained for a spin- $1/2$  pair with  $r \gg M$

$$T_{1OPF}^{-1} = (9/8)(\gamma^2 \hbar / r^3)^2 [kT v_N^{1/2} u(\omega/\omega_c) / 3\sqrt{2}\pi L N^{3/2} \omega^{1/2}] \{ [x(0,1)]^2 + 2\sqrt{2}[x(0,2)]^2 \} \quad (8)$$

and

$$T_{1Q} \text{ OPF}^{-1} = (9/8)(\gamma^2 \hbar / r^3)^2 \{ [kT v_N^{1/2} u(\omega/\omega_c) / 3\sqrt{2}\pi L N^{3/2} \omega^{1/2}] [5[x(0,1)]^2 / 2 + [x(0,2)]^2 / \sqrt{2}] + (kT/2\sqrt{2} Q) + N\epsilon [x(0,0)]^2 / L^2 N \} \quad (9)$$

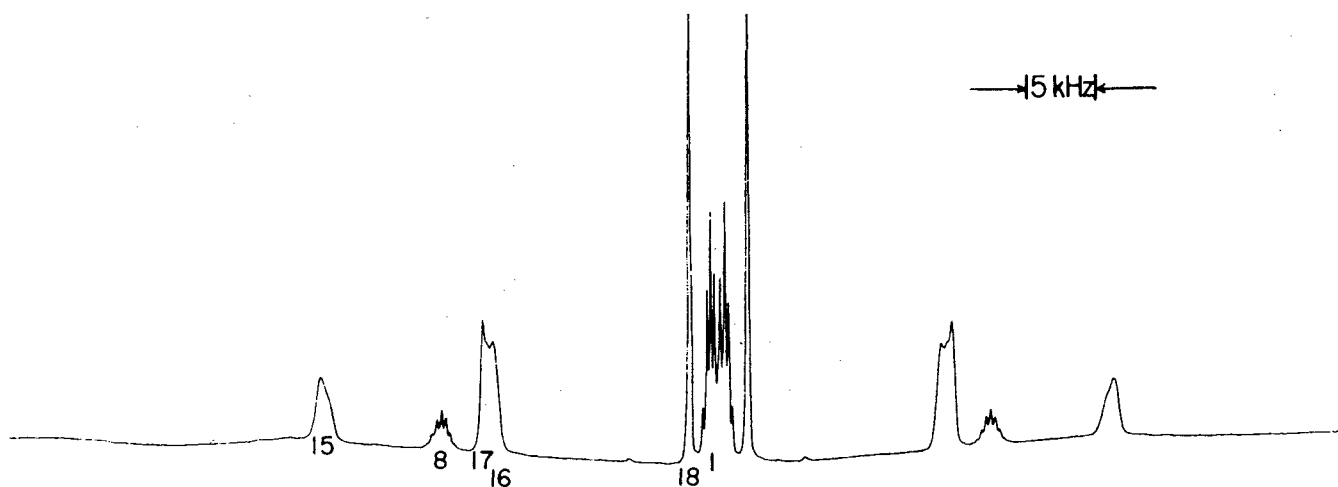
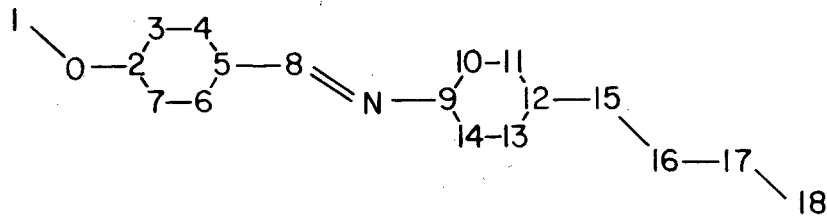


**Figure 3.** The structure of MBBA and a typical deuterium FFT spectrum of MBBA-d<sub>11</sub>. The carbon atoms of the methoxy group and the *n*-butyl chain are numbered as 1 and 15-18, respectively. H atoms are omitted for clarity. The doublets in the spectrum are labelled by the carbon atoms.

where  $\omega_1 \ll t_0 \ll \omega$  is assumed,  $\omega_1/\gamma$  is the rotating field  $B_1$ , and  $\xi = (LN/A)^{1/2}$  is the coherence length of the nematic order parameter fluctuations. The coefficients  $\alpha(0, M)$  are given (3) as a power series in  $S$  in (9), together with definitions of all other symbols. The last term in Eq. 9 comes from the spectral density  $J^{(0)}(2\omega_1)$  which is independent of  $B_1$  because  $\omega_1\tau \ll 1$  and acquires a critical dependence on temperature through the coherence length  $\xi$ . The quasi-critical OPF can therefore be detected by  $J^{(0)}(2\omega_1)$ . By combining Eqs. 8 and 9, one obtains

$$T_{1Q}^{-1} = T_{1Q} \text{OPF}^{-1} - f(S) T_{1\text{OPF}}^{-1} = \quad (10)$$

$$(9/8)(\gamma^2 \hbar / r^3)^2 (kT / 2\sqrt{2}\pi) [\alpha(0,0)]^2 v_N \xi / L_N^2$$

where

$$f(S) = [(5/2) + (1 - 5S/4)^2 / \sqrt{2}] / [1 + 4(1 - 5S/4)^2 / \sqrt{2}]$$

The problem of evaluating  $T_{1Q}'$  is in obtaining the quantities  $T_{1Q} \text{OPF}^{-1}$  and  $T_{1\text{OPF}}^{-1}$ . In our attempt (9) to search for OPF in PAA-d<sub>6</sub> at  $\omega = 60$  MHz, we made the following assumptions: (1)  $T_{1Q}^{-1} = T_{1Qa}^{-1}$ ; (2)  $T_{1r}^{-1} = T_{1a}^{-1} + T_{1r}^{-1} = 1.29 T_{1a}^{-1}$  for all temperatures and (3)  $T_{1a}^{-1} = T_{1\text{OPF}}^{-1}$  and  $T_{1Qa}^{-1} = T_{1Q} \text{OPF}^{-1}$  near  $T_c$ . The third assumption may be questionable since it has been shown that  $T_{1\text{AFS}}^{-1}$  at 60 MHz and 120°C makes a significant contribution to the total intramolecular relaxation rate. By analogy to Eq 2, one writes

$$T_{1Qa}^{-1} = T_{1Q} \text{OPF}^{-1} [1 - (2\sqrt{2}/\pi)(\omega\omega_c)^{1/2} \tau_R / U(\omega/\omega_c)] + T_{1Q\text{AFS}}^{-1} \quad (11)$$

where  $T_{1Q\text{AFS}}^{-1} = T_{1\text{AFS}}^{-1}$  is  $(1 + 3S/2)$  used. We will not discuss OPF further because a proper analysis of PAA-d<sub>6</sub> data still awaits further isotopic dilution ex-

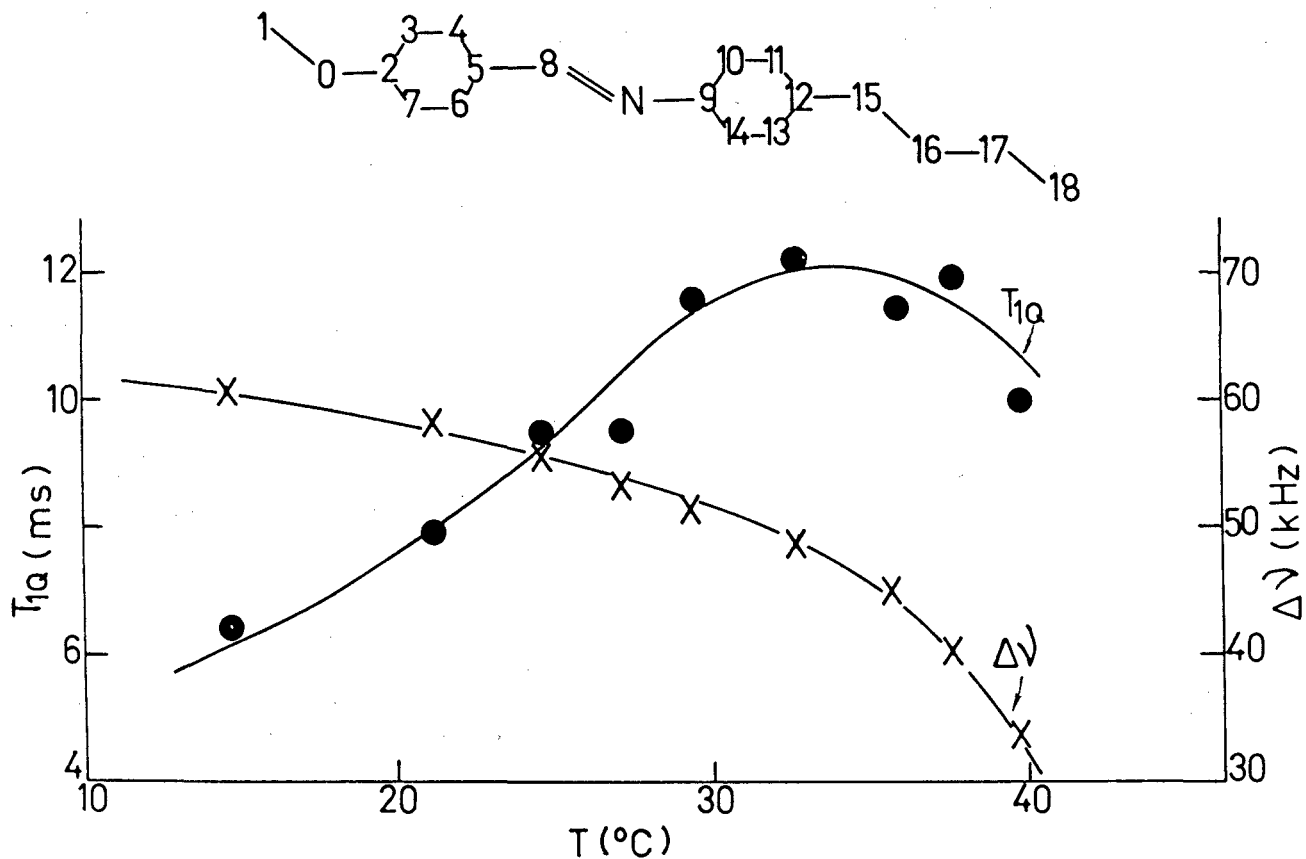


Figure 4. Plot of the deuteron relaxation time,  $T_{1\rho}$  and deuteron doublet splitting,  $\Delta\nu$ , for the carbon-15 deuterons vs temperature in the nematic phase of MBBA- $d_{13}$ .

periments in this system at temperatures near  $T_c$  from which  $T_{1\rho}^{-1}$  and  $\tau_R$  are experimentally determined.

### III. INTERMOLECULAR INTERACTION

Doane *et al* (2) give the following expression for the intermolecular proton relaxation rate, omitting the cross-relaxation term,

$$T_{1\rho}^{-1} = (9/4)(\gamma^2 \hbar^2 / r^3)^2 \{ [kTS^2 u(\omega/\omega_c) / 8\sqrt{2\pi} K(D + K/\eta)^{1/2} \omega^{1/2}] + (\tau_d/15)[2(1-S)/(1+W^2\tau_d^2) + (8+7S)/(1+4\omega^2\tau_d^2)] \} \quad (12)$$

where  $r$  is the distance between protons on different molecules, and  $\tau_d$  is the molecular jump correlation

time. The corresponding expression obtained by Zumer and Vilfan (10) is

$$T_{1\rho}^{-1} = (9/8)(\gamma^2 \hbar^2 / d^3) n \tau Q(\omega\tau, \langle r_{\perp}^2 \rangle / d^2, D_{\parallel}^{\circ} / D_{\perp}^{\circ}) \quad (13)$$

where  $n$  is the spin density,  $d$  the diameter of the rod-like molecules,  $\langle r_{\perp}^2 \rangle$  the mean square molecular jump length,  $D_{\parallel}^{\circ}$  and  $D_{\perp}^{\circ}$  the self-diffusion coefficients in the direction parallel and perpendicular, respectively, to the direction of the long molecular axis, and  $\tau = (\langle r_{\perp}^2 \rangle / d^2) \tau^{\circ}$  where  $\tau^{\circ}$  is defined by  $\tau^{\circ} = d^2 / 4D_{\perp}^{\circ}$ .  $Q$  is a dimensionless function which must be calculated numerically. Zumer and Vilfan (10) have calculated  $Q$  for the case  $d = 5\text{\AA}$ ,  $D_{\parallel}^{\circ} / D_{\perp}^{\circ} = 2$ , for different frequencies and three different values of the ratio  $\langle r_{\perp}^2 \rangle / d^2$ , viz, 1, 0.1, and 0.01.

In order to test experimentally the theories on the intermolecular proton spin-lattice relaxation, it is necessary to separate the measured relaxation rate into the intra- and intermolecular contributions. As mentioned before, one way of separation is to obtain  $T_{1a}^{-1}$  directly by the isotopic dilution technique. The other way is to calculate  $T_{1a}^{-1}$  theoretically. For the phenyl protons of MBBA-d<sub>13</sub>, we chose the latter

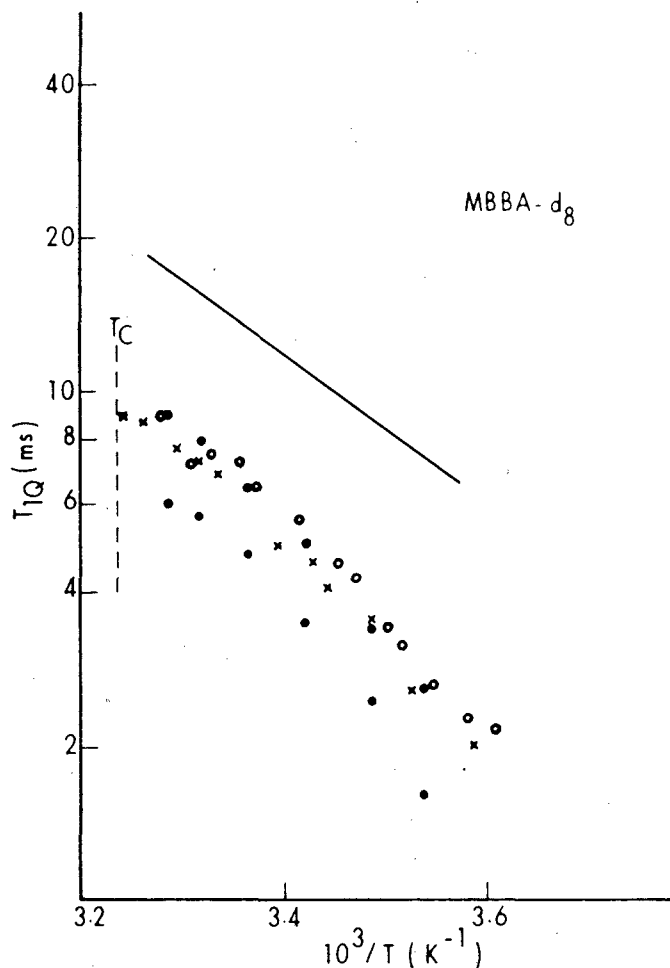


**Figure 5.** Deuteron spin-lattice relaxation time  $T_{1Q}$  of MBBA-d<sub>8</sub> vs the inverse of temperature. O and X denote measurements by Visintainer *et al* (6) at 9.21 and 4.5 MHz, respectively, and O denotes measurements by Rutar *et al* at 13.8 MHz. Solid line denotes theoretical plot at 13.8 MHz.

method. The proton  $T_{1r}^{-1}$  (Figure 6) was calculated (8) from Eq. 2 using the result in Figure 2 and the measured proton spin-lattice relaxation rate of

MBBA-d<sub>13</sub>. Figure 7 presents typical fits to the "experimental"  $T_{1r}^{-1}$  data at 29.2°C based on the above-mentioned theories. The lower curve is a theoretical plot of  $T_{1r}^{-1}$  vs  $\nu^{1/2}$  using Zumer and Vilfan's theory. We used  $n = 0.019/\text{Å}^3$ ,  $d = 5\text{Å}$ ,  $\langle r_{\perp}^2 \rangle / d^2 = 0.1$ , and  $\tau^0 = 3.47 \times 10^{-9}\text{s}$ . As seen in Figure 7, the agreement between theory and experiment is poor. The solid curve represents a fit to the experimental data using Eq. 12 with the adjustable parameters  $r$  and  $\tau_d$  equal to 2.85 Å and  $1.73 \times 10^{-9}\text{s}$ , respectively. We set  $u(\omega/\omega_c) = 1$  because the ODF contribution in this case is negligibly small in comparison with the AFS contribution. Now  $r$  remains essentially constant in the nematic range while  $\tau_d$ 's at different temperatures produce an activation energy of  $4.8 \pm 0.4$  kcal/mole. This compares favourably with the activation energy for self-diffusion (14) in MBBA found by Hervet *et al*, viz  $5.8 \pm 0.7$  kcal/mole for  $D_{\parallel}$  and  $6.0 \pm 0.8$  kcal/mole for  $D_{\perp}$ . The temperature dependence of  $T_{1r}^{-1}$  (Figure 6) at different frequencies can be reproduced quite well by the above  $\tau_d$  values. It would therefore seem that self diffusion is not the sole intermolecular contribution to the spin relaxation rate in MBBA, and the other relaxation mechanisms must also be present. If one assumes that the expression of Doane *et al* (2) for  $T_{1r}^{-1}$  accounts for the ODF and AFS only, and if one further assumes that these fluctuations are not coupled to self-diffusion, then the experimental  $T_{1r}^{-1}$  should be analyzed by the sum of Eqs. 12 and 13. Indeed, such an analysis is suggested by the frequency dependence of  $T_{1r}^{-1}$  in PAA (Figure 1). The dashed curve in the figure represents a fit with  $r = 2.91$  Å,  $\tau_d = 1.55 \times 10^{-9}\text{s}$ , and the self-diffusion contribution given by the lower curve. We note that the  $r$  and  $\tau_d$  do not vary significantly for the two fits, although the latter  $\tau_d$  values give an activation energy of  $6.5 \pm 0.3$  kcal/mole in closer agreement with that for self-diffusion.

Finally, the experimental  $T_{1r}^{-1}$  data of PAA-d<sub>6</sub> (Figure 1) at 120°C can be analyzed in exactly the same manner. In Figure 1, the lower dashed curve represents a plot given by Zumer and Vilfan's theory with  $n = 0.02/\text{Å}^3$ ,  $\langle r_{\perp}^2 \rangle / d^2 = 0.1$ ,  $d = 5\text{Å}$ , and  $\tau^0 = 2.08 \times 10^{-10}\text{s}$ . In the frequency range examined, self-diffusion are almost frequency independent. Again, the experimental  $T_{1r}^{-1}$  data is fitted by the sum of Eqs. 12 and 13. The solid curve represents the theory with  $r = 2.2$  Å,  $\tau_d = 1.64 \times 10^{-12}$  s, and the self-diffusion given by the dashed curve. In this case, the ODF con-

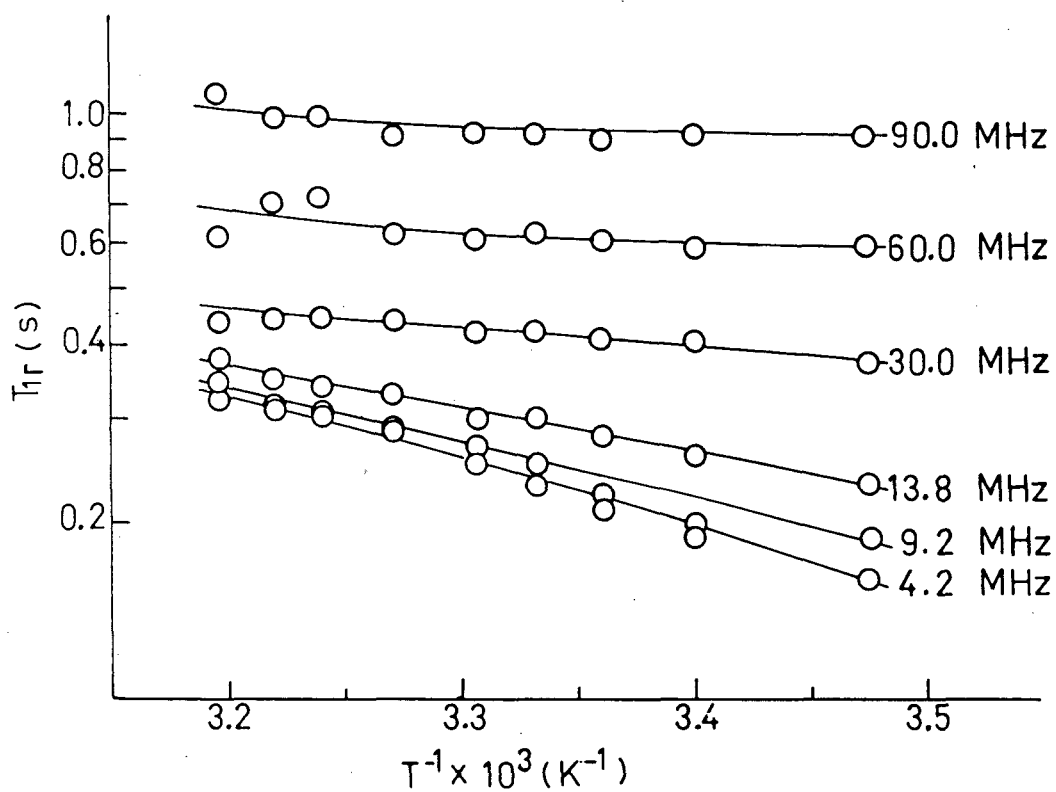
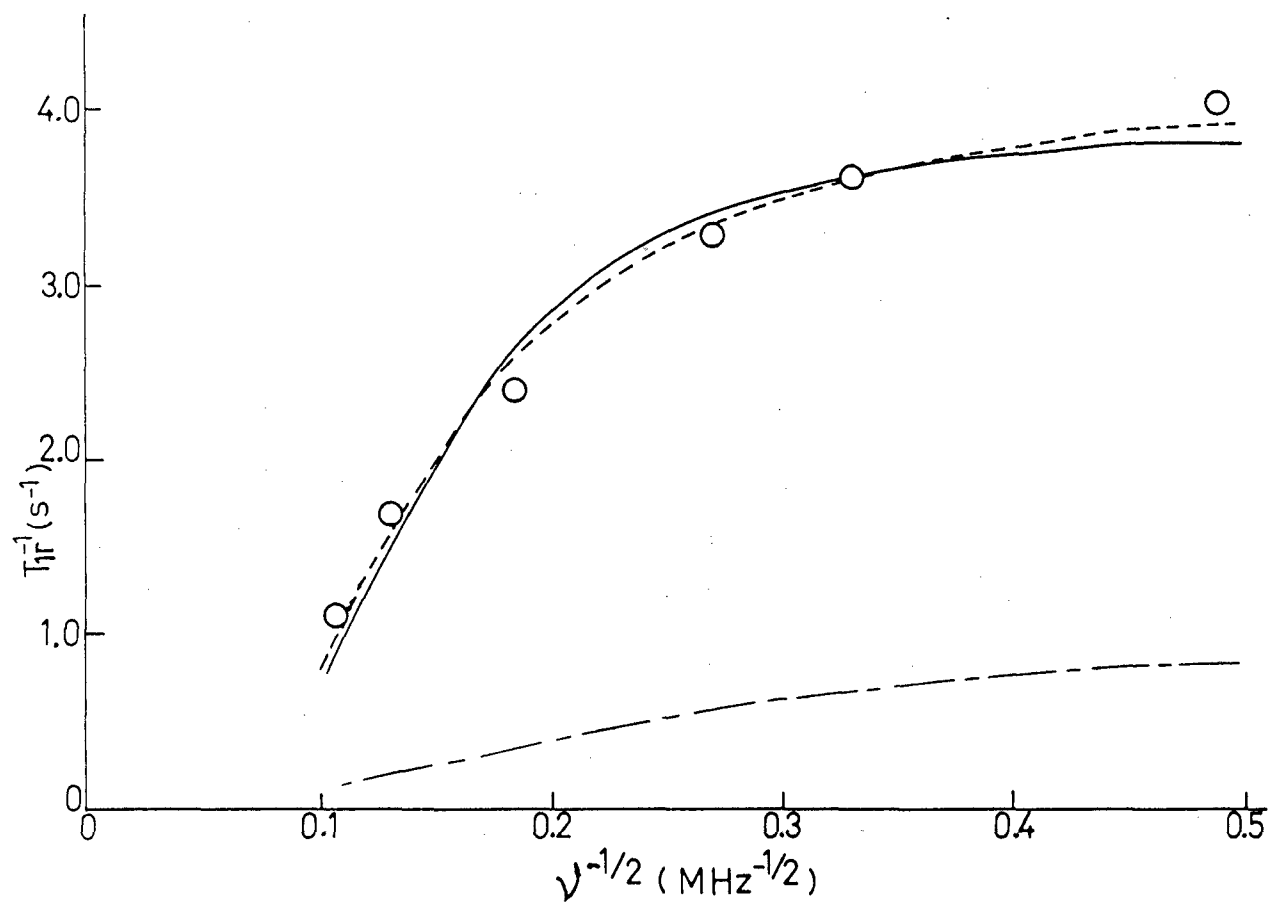


Figure 6. Intermolecular proton relaxation times of MBBA-d<sub>13</sub> at different temperatures and frequencies.

tribution dominates, and the AFS term is only 9% of the ODF contribution. Though  $\tau_d$  is smaller than that

estimated from the self-diffusion constant, the fit appears very good indeed.



**Figure 7.** Plot of the proton  $T_{1\rho}^{-1}$  vs  $\nu^{-1/2}$  for MBBA- $d_{13}$  at 29.2°C. The lower curve represents values from the theory of Zumer and Vilfan. Solid and dashed curves denote a fit to the data using, respectively, Doane's theory alone and the theories of both Doane *et al* and Zumer and Vilfan (see text).

## ACKNOWLEDGMENTS

Financial support of the National Research Council of Canada is gratefully acknowledged. Drs. E. Bock, J.S. Lewis, and E. Tomchuk are thanked for valuable discussions.

## REFERENCES

- <sup>1</sup>C.G. Wade, *Ann. Rev. Phys. Chem.* **28**, 47 (1977).  
<sup>2</sup>P. Ukleja, J. Pirs, and J.W. Doane, *Phys. Rev. A* **17**, 414 (1976) and references therein.  
<sup>3</sup>J. Freed, *J. Chem. Phys.* **66**, 4183 (1977).  
<sup>4</sup>W. Wolfel, F. Noack, and M. Stohrer, *Z. Naturforsch.* **A30**, (1975) and references therein.  
<sup>5</sup>V. Graf, F. Noack, and M. Stohrer, *Z. Naturforsch.* **A32**, 61 (1977) and references therein.

- <sup>6</sup>J.J. Visintainer, R.Y. Dong, E. Bock, E. Tomchuk, D.B. Dewey, A.L. Kuo, and C.G. Wade, *J. Chem. Phys.* **66**, 3343 (1977).  
<sup>7</sup>R.Y. Dong, J. Lewis, E. Tomchuk, and E. Bock, *J. Chem. Phys.* **69**, 5314 (1978).  
<sup>8</sup>R.Y. Dong, E. Bock, J.S. Lewis and E. Tomchuk, *J. Chem. Phys.*, **72**, 5014 (1980).  
<sup>9</sup>R.Y. Dong and E. Tomchuk, *Phys. Rev. A* **17**, 2062 (1978).  
<sup>10</sup>S. Zumer and M. Vilfan, *Phys. Rev. A* **17**, 424 (1978); *J. Mol. Struct.* **46**, 475 (1978).  
<sup>11</sup>B.M. Fung, C.G. Wade, and R.D. Orwoll, *J. Chem. Phys.* **64**, 148 (1976).  
<sup>12</sup>R.D. Orwoll, C.G. Wade, and B.M. Fung, *J. Chem. Phys.* **63**, 986 (1975).  
<sup>13</sup>V. Rutar, M. Vilfan, R. Blinc, and E. Bock, *Mol. Phys.* **35**, 721 (1978).  
<sup>14</sup>Y.S. Lee, Y.Y. Hsu, and D. Dolphin in *Liq. Cryst. and Ordered Fluids*, J.F. Johnson and R.S. Porter, Eds., Plenum Press, New York, 1974, Vol. 2, p. 357; S. Meiboom and R.C. Hewitt, *Phys. Rev. Lett.* **30**, 261 (1972); I. Haller, *J. Chem. Phys.* **57**, 1400 (1970); H. Hervet, W. Urback, and F. Rondelez, *J. Chem. Phys.* **68**, 2727 (1978).